Surface Metal-Insulator Transition on a Vanadium Pentoxide (001) Single Crystal

R.-P Blum,[1,2] H. Niehus,[2] C. Hucho,[3] R. Fortrie,[4] M. V. Ganduglia-Pirovano,[4] J. Sauer,[4]
S. Shaikhutdinov,[1] and H.-J. Freund[1]

[1]*Fritz-Haber-Institut der Max-Planck-Gesellschaft, Faradayweg 4-6, Berlin 14195, Germany*
[2]*Institut für Physik, Humboldt Universität zu Berlin, Newtonstraße 15, Berlin 12489, Germany*
[3]*Paul-Drude-Institut für Festkörperelektronik, Hausvogteiplatz 5-7, Berlin 10117, Germany*
[4]*Institut für Chemie, Humboldt Universität zu Berlin, Unter den Linden 6, Berlin 10099, Germany*
(Received 25 May 2007; published 28 November 2007)

In situ band gap mapping of the $V_2O_5(001)$ crystal surface revealed a reversible metal-to-insulator transition at 350–400 K, which occurs inhomogeneously across the surface and expands preferentially in the direction of the vanadyl ($V = O$) double rows. Supported by density functional theory and Monte Carlo simulations, the results are rationalized on the basis of the anisotropic growth of vanadyl-oxygen vacancies and a concomitant oxygen loss driven metal-to-insulator transition at the surface. At elevated temperatures irreversible surface reduction proceeds sequentially as $V_2O_5(001) \rightarrow V_6O_{13}(001) \rightarrow V_2O_3(0001)$.

Vanadium oxides represent an important class of materials with high potential in many technological applications based on their diverse temperature-dependent electronic, magnetic, and catalytic properties (e.g., [1–4] and references therein). There is a large variety of the vanadium oxide phases such as VO (V^{+2}, rocksalt structure), V_2O_3 (V^{+3}, corundum), VO_2 (V^{+4}, rutile), V_2O_5 (V^{+5}, layered orthorhombic), etc. Depending on the ambient conditions and temperature, phase transformations between these oxides can occur. They may involve the formation of mixed valence phases. In addition, several vanadium oxides undergo metal-to-insulator transitions (MIT), e.g., V_2O_3 at ~150 K, VO_2 at ~340 K. These complex structural and electronic transformations may play a crucial role in the behavior of vanadia-based systems.

Among the surface structures of vanadium oxides [4], the $V_2O_5(001)$ surface seems to be the most studied [3,5–12]. This surface exposes vanadyl ($V = O$) double rows along the [010] direction [Fig. 1(a)], which were observed also with scanning tunneling microscopy (STM) [10,11] and atomic force microscopy [12]. Surprisingly, the $V = O$ termination has been found also for the most stable, (0001) surface of V_2O_3 [4,13,14], whereas the $VO_2(110)$ surface appears to follow the respective bulk termination [1,4,15,16].

Since the thermally induced transformations of vanadium oxides may be initiated at the surface and even be restricted to the surface layers, it is important to study their surface structures in the early stages of transitions when several structures may coexist. In this respect, STM combined with scanning tunneling spectroscopy (STS) can provide direct information on both geometrical and electronic structures of oxide surfaces (see, e.g., [17]). We here report thermally induced reconstructions observed by STM/STS on a $V_2O_5(001)$ single crystal surface. Data show that V_2O_5, which is not known for the MIT in the bulk, exhibits, however, the MIT at the surface which

proceeds through the formation and anisotropic growth of vanadyl-oxygen vacancies and is followed by an irreversible surface reduction. The experimental findings are supported by density functional theory (DFT) and
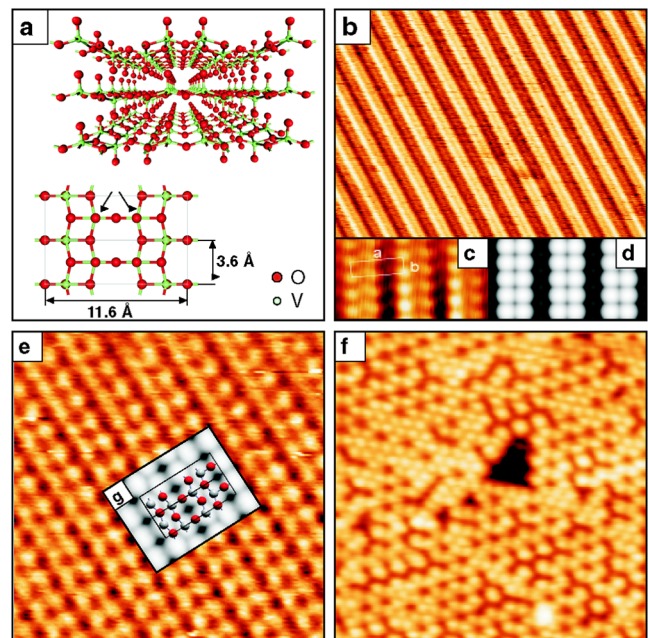

FIG. 1 (color online). (a) Perspective and top views of $V_2O_5(001)$. The unit cell is indicated. The arrows indicate the vanadyl ($V = O$) species. (b) STM image (15×15 nm², −1.1 V, 0.45 nA) of the vacuum-cleaved $V_2O_5(001)$ surface at 300 K showing double rows structure. (c) High-resolution STM image (4×2 nm², −1.1 V, 0.45 nA). (d), (g) Simulated STM image of the occupied (V_2O_5) and unoccupied (V_6O_{13}) states based on DFT calculations. (e), (f) STM images of the V_2O_5 single crystal surface after flashing once to 800 K (5×5 nm², +0.18 V, 0.3 nA) and after several flashes to 800 K (15×15 nm², −1.3 V, 0.3 nA), respectively.

Monte Carlo calculations. The results may have strong impact both on catalysis and material science of vanadium oxides if the morphologies involve nanoparticles and ultra-thin films.

The experiments were performed in ultrahigh vacuum (UHV, base pressure $<2 \times 10^{-10}$ mbar) chamber equipped with STM, low energy electron diffraction (LEED), and x-ray photoelectron spectroscopy (XPS). The $V_2O_5(001)$ single crystal ($10 \times 4 \times 4$ mm^3) was grown as described elsewhere [18]. The crystal was cleaved in UHV using adhesive tape. The LEED and XPS measurements were performed *after* STM studies in order to avoid electron induced damaging effects [5].

A freshly cleaved crystal surface exposed very large terraces (up to few μm in width) separated by monoatomic steps of ~4 Å in height. Figures 1(b) and 1(c) show STM images of the $V_2O_5(001)$ surface at room temperature, where the protrusions can be assigned straightforwardly to the vanadyl [19] [Fig. 1(d)]. While heating the sample up to 350 K and simultaneously monitoring the surface to-pography by STM we observed, in addition to the rowlike structure (labeled *A* in Fig. 2), domains with an apparently flat surface (labeled *B*), the area of which increases further while heating up to 400 K.

Structure *A* exhibits rows with an ~11 Å spacing similar to those observed on the pristine $V_2O_5(001)$ surface at 300 K [Fig. 1(b)], although atomic resolution has not been achieved. The tunneling spectra measured in several points over these *A* regions revealed, however, an average band gap of ~0.6 eV, which is much smaller than that measured on $V_2O_5(001)$ at 300 K [~1.8 eV, Fig. 2(b)]. In contrast, *B* domains show spectra which are characteristic for metallic surfaces, which may explain a low corrugation amplitude reached on these domains.

Band gap maps derived from STS data (one spectrum per ~1 nm^2) are shown in Fig. 2. At 350 K, the domains with a metallic conductivity basically coincide with the *B* domains imaged by STM, as can be seen in Fig. 2(c), and appear mostly as slightly elongated islands. At 400 K, the *B* domains coalesce and increase in area without significant changes in the tunneling spectra. The original surface topography and tunneling spectra of $V_2O_5(001)$ are fully recovered after cooling the sample back to the room tem-perature. Finally, XPS measurements at 300 K did not show any changes in the V3d and O1s core levels unless the sample is heated up to 800 K (see below).

Therefore, the STM/STS results show that the $V_2O_5(001)$ crystal surface in UHV undergoes a reversible restructuring resulting in the MIT, which must be limited to the surface layer(s) only since the bulk V_2O_5 does not exhibit the MIT. It is known that the V_6O_{13} phase, which is formed from the O-defective V_2O_5 phase by applying a crystallographic shear operation [2,5,6], exhibits a metallic behavior above 150 K [20]. The structural similarity be-tween these two phases is obvious considering their re-spective unit cells (V_2O_5: **a** = 11.5 Å, **b** = 3.56 Å.
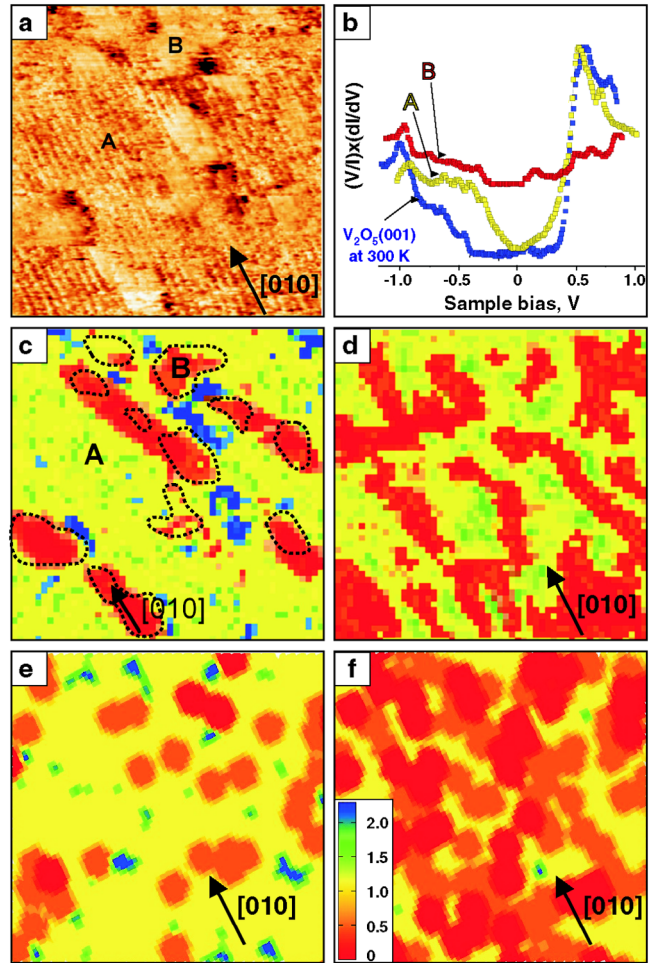

FIG. 2 (color online). (a) STM image (50×50 nm^2, -1.3 V, 0.24 nA) of the $V_2O_5(001)$ surface at 350 K. (b) Normalized conductance spectra over areas *A* and *B* at 350 K, and over $V_2O_5(001)$ at 300 K. (c), (d) Band gap maps of the surface recorded at 350 K (c) and 400 K (d). The contours of the *B* domains as imaged in (a) are superimposed with the band map on (c). (e), (f) Simulated gap maps at 300 K for different simulation conditions (see text). The band gap scale (in eV) is indicated.

V_6O_{13}: **a** = 11.9 Å, **b** = 3.68 Å). As a consequence, *B* domains could, in principle, be assigned to the first stages of the $V_2O_5 \rightarrow V_6O_{13}$ phase transition.

In order to rationalize the STS spectra [Fig. 2(b)] we performed DFT + U calculations for the clean as well as defective $V_2O_5(001)$ surfaces containing either isolated vanadyl-oxygen defects or missing vanadyl-oxygen rows [21]. It is not expected that plain DFT with GGA-type functionals adequately describe the electronic properties of reduced transition metal oxide systems [22].

The DFT + U calculated density of states (DOS) of the clean $V_2O_5(001)$ surface yields a band gap of ~2.3 eV (Fig. 3), which is similar to the measured value of ~1.8 eV [Fig. 2(b)]. The formation of isolated surface defects re-sults in the reduction of the band gap down to ~1.1 eV. The removal of any outmost vanadyl oxygen leads to
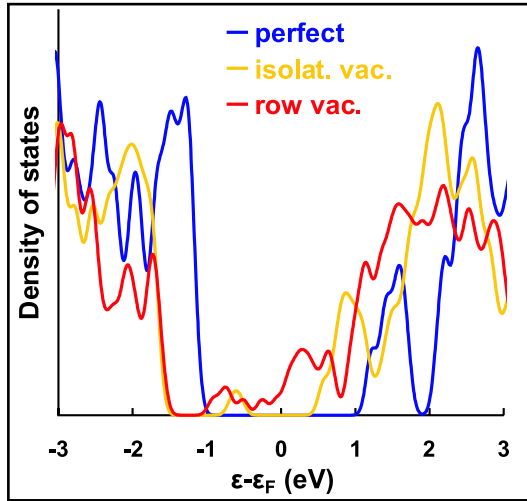
FIG. 3 (color online).   Calculated density of states of the clean $V_2O_5(001)$ surface (blue, for online version), of the defective surface containing isolated vanadyl-oxygen vacancies (yellow), and of the missing-row structure (red). The curves are smoothed by a Gaussian level broadening of 0.2 eV.

significant lattice relaxation resulting in the formation of a V^{4+}-O-V^{4+} bond between the surface vanadium site (after removal of the vanadyl oxygen) and the vanadyl group of the layer beneath [19,23]. The excess electrons localize at the V sites involved in the interlayer bonding and occupy V3d states that are split from the bottom of the conduction band. As a consequence, the band gap is reduced. For the missing-row structure, the metallic character is clearly observed (see Fig. 3). The DFT + U calculated DOS of $V_6O_{13}(001)$ also exhibits metallic character [24].

Earlier plain DFT calculations of reduced $V_2O_5(001)$ surfaces indicated that, starting from isolated vanadyl-oxygen defect, the defect formation energy of subsequent oxygen vacancies decreases with increasing number of neighboring defects along the vanadyl rows, and a facile reduction along the [010] direction was predicted [19]. These results suggest that the A domains may be attributed to a partially reduced $V_2O_5(001)$ surface with randomly distributed isolated vacancies, whereas the B domains are attributed to the missing-row phase with trenches of various lengths.

In order to see whether distributions like those shown in Fig. 2(c) and 2(d) are compatible with this assignment, we employ Monte Carlo simulations as follows. The $V_2O_5(001)$ surface is modeled with the 2D-periodic network represented in Fig. 4, each node being occupied by a vanadyl site or a vanadyl-oxygen defect site. Five pairwise interaction parameters, fitted to the DFT energies of Ref. [19], describe the interactions between vanadyl-oxygen defect sites (Fig. 4).

The network consists of 50 double rows of 2×150 sites, which corresponds to an area of 57.75×53.7 nm^2. Ten trajectories, starting from random states, are simulated using the METROPOLIS algorithm [25] for a varying fraction
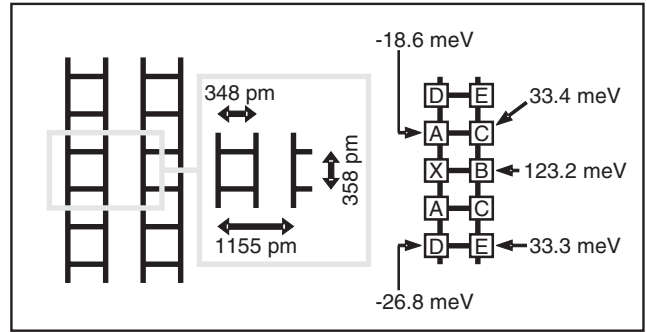

FIG. 4.   (Left) 2D-periodic network used for Monte Carlo simulations. Each node is occupied by a reduced or oxidized vanadyl termination. (Middle) Geometrical characteristics of the network. (Right) Interaction parameters between a given reduced site (X) and other reduced sites.

of reduced sites (0%–100%, every 2.5%). The resulting uncertainty on the average energy is lower than 0.05 meV, which proves that the system is well thermalized. At the experimental conditions ($<10^{-10}$ mbar of O_2), the fraction of reduced sites is approximately 2.6% and 3.1% at 350 and 400 K, respectively. To compare the predicted distribution of reduced sites with the experimental data, two particular states of the partially reduced surface were considered and the corresponding gap maps were modeled as follows. Each local electronic state was assumed to be felt by the STM tip over the area with a radius of 2.78 nm. The gap value was taken equal to the smallest gap within that radius.

Figures 2(e) and 2(f) show the results of MC simulation run at 300 K for 3% [Fig. 2(e)] and 7% [Fig. 2(f)]of reduced sites. Both experimental and calculated band gap maps exhibit a disordered pattern with almost the same amount of each color. [The upper part of Fig. 2(c) shows an elongated stripe missing in Fig. 2(e), which in fact results from an accidental accumulation of several [010] oriented "border sharing" smaller domains.] Note that kinetic effects that may favor the formation of longer defective rows and thermal drift (which may influence experimental data) were not considered in the simulation.

Heating to elevated temperatures leads to the formation of $V_6O_{13}(001)$ in the first and to $V_2O_3(001)$ in the second stage as revealed by STM (see Fig. 1). These phase transformations occur only within the surface layers, whereas deeper layers maintain the V_2O_5 crystal structure (see supporting information [26]). After the first heating to 800 K, the STM images fit well the $V_6O_{13}(001)$ surface [Fig. 1(e)]. The protrusions in these images, recorded for the empty states basically comprising the V3d orbitals [24], show the positions of the V cations in the surface layer. It seems plausible that during fast heating to 800 K, vanadyl oxygen is desorbed from the surface region, which cannot be replenished due to the low diffusion from the bulk. As a result, the O-deficient $V_2O_5(001)$ surface reconstructs into $V_6O_{13}(001)$, which indeed does not require

strong atom displacements. There seems to be a critical concentration of the oxygen vacancies for the phase transformation to occur.

The STM images from the more reduced surface [see Fig. 1(f)] are in fact very similar to those reported for $V_2O_3(0001)$ films [4] and therefore consistent with the observation of V^{3+} species by XPS (not shown).

Full analysis of the stability plot for the different vanadia surfaces considered here as a function of temperature and oxygen pressure (see supporting information [26]) revealed that the defective V_2O_5 surface is the most stable phase at 350 K. At 400 K the defective V_2O_5 surface remains the most stable phase; however, the defect concentration increases and defects form the missing vanadyl rows of various length. At 800 K the V_6O_{13} and vanadyl terminated V_2O_3 phases become more stable than V_2O_5. As a result, the V_2O_5 to V_6O_{13} and/or to V_2O_3 phase transition is predicted as indeed observed by STM (see Fig. 1). This scenario is rationalized on the basis of thermodynamic data only. However, this does not provide information on the kinetics, i.e., under which circumstances reversibility occurs. This issue needs to be further studied.

In summary, using *in situ* STM and band gap mapping, derived from scanning tunneling spectroscopy data, we have observed a metal-to-insulator transition of the $V_2O_5(001)$ single crystal at 350–400 K, which is restricted to the surface layers and occurs anisotropically across the surface. These findings are rationalized with the help of DFT and Monte Carlo simulations, on the basis of the formation of vanadyl-oxygen vacancies which preferentially grow along the vanadyl rows. Heating to elevated temperatures (800 K) leads to irreversible surface reduction which proceeds sequentially $V_2O_5(001) \rightarrow V_6O_{13}(001) \rightarrow V_2O_3(0001)$, as observed by high-resolution STM.

[1] V. E. Henrich and P. A. Cox, *The Surface Science of Metal Oxides* (Cambridge University Press, Cambridge, England, 1994).

[2] J. Haber, M. Witko, and R. Tokarz, Appl. Catal., A **157**, 3 (1997).

[3] K. Hermann and M. Witko, in *The Chemical Physics of Solid Surfaces: Oxide Surfaces*, edited by D. P. Woodruff (Elsevier, New York, 2001), Vol. 9.

[4] S. Surnev, M. G. Ramsey, and F. P. Netzer, Prog. Surf. Sci. **73**, 117 (2003).

[5] M. N. Colpaert, P. Clauws, L. Fiermans, and J. Vennik, Surf. Sci. **36**, 513 (1973).

[6] K. Devriendt, H. Poelman, and L. Fiermans, Surf. Sci. **433–435**, 734 (1999).

[7] S. Shin, S. Suga, and M. Taniguchi *et al.*, Phys. Rev. B **41**, 4993 (1990).

[8] R. Eguchi, T. Yokoya, and T. Kiss *et al.* Phys. Rev. B **65**, 205124 (2002).

[9] M. Demeter, M. Neumann, and W. Reichelt, Surf. Sci. **454–456**, 41 (2000).

[10] T. Oshio, Y. Sakai, and S. Ehara, J. Vac. Sci. Technol. B **12**, 2055 (1994).

[11] R. A. Goschke, K. Vey, and M. Maier *et al.*, Surf. Sci. **348**, 305 (1996).

[12] R. L. Smith, G. S. Rohrer, and K. S. Lee *et al.*, Surf. Sci. **367**, 87 (1996).

[13] A.-C. Dupuis, M. Abu Al-Haija, and B. Richter *et al.*, Surf. Sci. **539**, 99 (2003).

[14] F. Pfuner, J. Schoiswohl, and M. Sock *et al.*, J. Phys. Condens. Matter **17**, 4035 (2005).

[15] M. Sambi, M. Della Negra, and G. Granozzi, Surf. Sci. Lett. **470**, L116 (2000).

[16] J. Middeke, R.-P. Blum, M. Hafemeister, and H. Niehus, Surf. Sci. **587**, 219 (2005).

[17] K. McElroy, J. Lee, and J. A. Slezak *et al.*, Science **309**, 1048 (2005).

[18] F. Jachmann and C. Hucho, Solid State Commun. **135**, 440 (2005).

[19] M. V. Ganduglia-Pirovano and J. Sauer, Phys. Rev. B **70**, 045422 (2004).

[20] K. Kawashima, Y. Ueda, K. Kosuge, and S. Kachi, J. Cryst. Growth **26**, 321 (1974).

[21] The DFT + U calculations were performed using the VASP [27] package and the PW91 exchange-correlation functional [28]. The clean and defective surfaces are modeled using a two layer (001) oriented slab and (1 × 1) and (1 × 3) unit cells, respectively. The value of $U = 3$ eV used provides good agreement for a number of properties of vanadium oxides [22].

[22] M. V. Ganduglia-Pirovano, A. Hofmann, and J. Sauer, Surf. Sci. Rep. **62**, 219 (2007).

[23] K. Hermann, M. Witko, R. Druzinic, and R. Tokarz, Appl. Phys. A **72**, 429 (2001).

[24] R. Fortrie, M. V. Ganduglia-Pirovano, and J. Sauer *et al.* (to be published).

[25] N. Metropolis, A. W. Rosenbluth, and M. N. Rosenbluth *et al.*, J. Chem. Phys. **21**, 1087 (1953).

[26] See EPAPS Document No. E-PRLTAO-99-063748 for supporting information. For more information on EPAPS, see http://www.aip.org/pubservs/epaps.html.

[27] G. Kresse and J. Hafner, Phys. Rev. B **48**, 13 115 (1993); G. Kresse and J. Furthmüller *ibid.* **54**, 11 169 (1996).

[28] J. P. Perdew *et al.*, Phys. Rev. B **46**, 6671 (1992).